REQUEST FOR A SPECIAL PROJECT 2016–2018

MEMBER STATE: Germany

Principal Investigator[1]: Prof. Dr. George Craig

Affiliation: Meteorologisches Institut, Ludwig-Maximilian-Universität

Address: Theresienstraße 37
80333 München

E-mail: george.craig@lmu.de

Other researchers: Dr. Tobias Selz (tobias.selz@lmu.de),
Prof. Volkmar Wirth
Dr. Michael Riemer

Project Title: Upscale impact of diabatic processes from convective to near-hemispheric scale (as part of the Waves to Weather project)

If this is a continuation of an existing project, please state the computer project account assigned previously.	**SP** __________________	
Starting year: (Each project will have a well defined duration, up to a maximum of 3 years, agreed at the beginning of the project.)	2016	
Would you accept support for 1 year only, if necessary?	YES ☒	NO ☐

Computer resources required for 2016-2018: (The maximum project duration is 3 years, therefore a continuation project cannot request resources for 2018.)	**2016**	**2017**	**2018**
High Performance Computing Facility (units)	2.5M	2.5M	2.5M
Data storage capacity (total archive volume) (gigabytes)	500	500	500

*An electronic copy of this form **must be sent** via e-mail to:* *special_projects@ecmwf.int*

Electronic copy of the form sent on (please specify date): 1.7.2015

Continue overleaf

1The Principal Investigator will act as contact person for this Special Project and, in particular, will be asked to register the project, provide an annual progress report of the project's activities, etc.

Principal Investigator: George Craig

Project Title: Upscale impact of diabatic processes from convective to near-hemispheric scale

Extended abstract

This Special Project is closely linked to the subproject A1 “Upscale impact of diabatic processes from convective to near-hemispheric scale” of the recently funded DFG-Collaborative Research Center “Waves to Weather”, in which ECMWF and DWD are also involved as cooperation partners. As an extended abstract the relevant parts of the A1-proposal are attached, which contain a detailed workplan and a comprehensive description of the project motivation. The project is funded by DFG without any modification.

Justification of requested computer resources

It is planned to use the ICON model (the new global model of DWD) together with the Plant-Craig convection scheme to assess the practical importance of upscale error growth from convection. Altogether the simulation of 8 different cases is planned over the three years, with ensemble size of 40 members and forecast lead times up to 10 days, giving 4000 forecast days.

The aim is to use a R03B06 resolution (30km), since the Plant-Craig scheme has been shown to simulate basic properties of upscale error growth well in this setup (Selz and Craig, 2015b). A small test showed that the ICON model uses 1882 SBUs per forecast day at this resolution. The additional cost of the Plant-Craig scheme is estimated with 25%, giving 2353 SBUs per forecast day or 7.5 MSBUs altogether, distributed among the three years.

The simulation data will be transferred to a local data server and processed by local computing resources. We request a small amount of data storage at ECMWF to save restart files of the simulations, to enable extensions of the forecast, if appropriate.

Selz, T., and G. C. Craig (2015b), Simulation of upscale error growth with a stochastic convection scheme, Geophys. Res. Lett., 42, doi:10.1002/2015GL063525.

Technical characteristics of the code

The ICON model is written in Fortran90 and uses both shared memory multiprocessing (via OpenMP) and distributed memory parallelization (via MPI). DWD is already running ICON on the ECMWF supercomputer by and a close cooperation to the scientists at DWD will ensure that the code is used in the most efficient way.

A1 Upscale impact of diabatic processes from convective to near-hemispheric scale

A1.1 Basic information

A1.1.1 Principal investigator(s)

Prof. Dr. George C. Craig,
Meteorologisches Institut, Ludwig-Maximilians-Universität,
Theresienstr. 37, 80333 München, Germany
phone: +49 89 2180-4570; e-mail: george.craig@lmu.de

Prof. Dr. Volkmar Wirth,
Institut für Physik der Atmosphäre, Johannes Gutenberg-Universität Mainz,
Becherweg 21, 55128 Mainz, Germany
phone: +49 6131 39-22868; e-mail: vwirth@uni-mainz.de

Dr. Michael Riemer,
Institut für Physik der Atmosphäre, Johannes Gutenberg-Universität Mainz,
Becherweg 21, 55128 Mainz, Germany
phone: +49 6131 39-20027; e-mail: mriemer@uni-mainz.de

A1.2 Summary

In this project we will investigate the process of upscale propagation of uncertainty in the atmosphere over three orders of magnitude in spatial scale, from convective clouds to hemispheric waves. This will be possible by combining expertise of three partners at two universities and take advantage of recent developments in numerical atmospheric modeling (ICON) and stochastic parameterization (Plant-Craig). The non-hydrostatic ICON model allows for local grid refinements while the Plant-Craig convection scheme is able to emulate convective uncertainty at non-convective permitting resolutions. These two tools will form the basis for a series of error growth experiments to address open questions about basic characteristics, mechanisms and the practical importance of upscale error growth in mid-range global weather prediction. Diagnostic tools already successfully applied in uncertainty propagation studies will be further developed and jointly applied to the considered cases to attribute physical processes to error growth and improve our understanding of sources and limitations of atmospheric predictability. A novel diagnostic will be developed which allows one to diagnose wave activity for finite amplitude Rossby wave packets; it will be applied in order to quantify forecast errors and ensemble spread on the large-scale end of the spectrum. This project will also contribute to a better conceptual understanding of the relation between two seemingly distinct perspectives on balanced dynamics, namely potential vorticity thinking and the wave activity framework. We will cooperate with visualization projects to facilitate the handling of five-dimensional ensemble data and extracting the relevant information.

A1.3 Research rationale

A1.3.1 Current state of understanding

There are primarily two phenomena that lead to a limitation of the predictability of midlatitude weather systems on synoptic scales. First, there is the uncertainty of the initial, synoptic-scale state itself that grows due to processes intrinsic to the dynamics and eventually results in errors that reach the amplitude of the climate variability. Second, processes on smaller scales with much shorter inherent predictability can grow upscale and introduce additional uncertainties into the balanced flow that limit its predictability even if the initial state was perfectly known.

For synoptic-scale dynamics one can, again, distinguish two basic processes which contribute to uncertainty growth. One is baroclinic instability, which leads to exponential growth of wave amplitudes on the scale of a few days (Eady, 1949). Unsurprisingly, this mechanisms is associated with the growth of errors on the same time scale (Zhang et al., 2007). A second mechanism is related to the nonlinearity of the flow and wavebreaking, which is sometimes associated with strong sensitivity to initial conditions and bifurcation-like behavior even in the absence of baroclinic instability. Quite recently Riemer and Jones (2014) have shown that this mechanism can imply substantial error growth.

For upscale error growth, Zhang et al. (2007) presented a three stage conceptual model derived from an idealized case study. The first stage describes convective-scale error growth, where the initial perturbation energy on scales up to 200 km doubles on the order of an hour. In regions with moist convection, this growth rate is further increased and after a few hours significant error structures are basically confined to these regions (Hohenegger and Schär, 2007b). Consequently, the intrinsic predictability of convective processes is by a factor of ten lower than for the geostrophic dynamics (Hohenegger and Schär, 2007a). The fast initial growth however slows down quickly and finally saturates on the order of 12 hours, leading to a complete or random displacement of individual convective cells. The resulting variability in upper level divergence and gravity wave propagation introduce geostrophic adjustment processes, propagating the errors onto larger scales and getting them into geostrophic balance (stage two). In stage three, this balanced, small-amplitude perturbation grows further, now directly driven by synoptic-scale instabilities as for synoptic-scale uncertainty in the initial state. Selz and Craig (2015) recently showed that this conceptual model could be applied to a real summertime weather event over Europe.

Zhang et al. (2007) argued that the *intrinsic* predictability of the synoptic-scale flow is limited by upscale error growth from convective instability. There is, however, a controversy about its *practical* importance. Durran and Gingrich (2014) pointed out that due to the underlying kinetic energy spectrum of the atmosphere a small relative uncertainty in the initial state on large scales is still in amplitude much larger than a big relative error on smaller scales. On the other hand Rodwell et al. (2013) showed a relation between periods with bad forecasts over Europe and high convective activity upstream over the North-American continent. This indicates that the importance of upscale error growth is probably regime-dependent, being negligible in one case but with significant impact in another. It is therefore important to understand the processes of upscale error growth in more detail and investigate their representation in numerical weather models.

An important framework to understand the processes that govern the generation and evolution of forecast errors is provided by potential vorticity (PV) and its material rate of change. PV errors exhibit a maximum amplitude along the midlatitude, upper-tropospheric waveguide (Dirren et al., 2003). Diabatic contributions to these errors and structural characteristics of the diabatically-generated error has been studied in some detail (Chagnon et al., 2013; Gray et al., 2014). However, recent work has identified a second mechanism, in addition to diabatic PV generation, through which latent heat release generates forecast errors. Mid-tropospheric latent heat release is usually associated with strong divergent outflow near the tropopause. Displacements of the strong midlatitude PV gradient by this divergent flow has been demonstrated for tropical cyclones undergoing extratropical transition (e. g., Riemer et al., 2008; Grams et al., 2013; Archambault et al., 2013), mesoscale convective systems (Rodwell et al., 2013), and warm conveyor belts associated with extratropical cyclones (Grams et al., 2011). Errors in the divergent flow thus lead to distinct PV errors by erroneous displacements of the PV gradient. Subsequent to their generation, a qualitative description of the error evolution in terms of PV conservation and PV invertability has proven insightful (Rodwell et al., 2013).

For a quantitative analysis, Davies and Didone (2013) derived an equation for the tendency of the PV error following the analyzed flow [their Eq. (6)]. Their equation distinguishes advective and

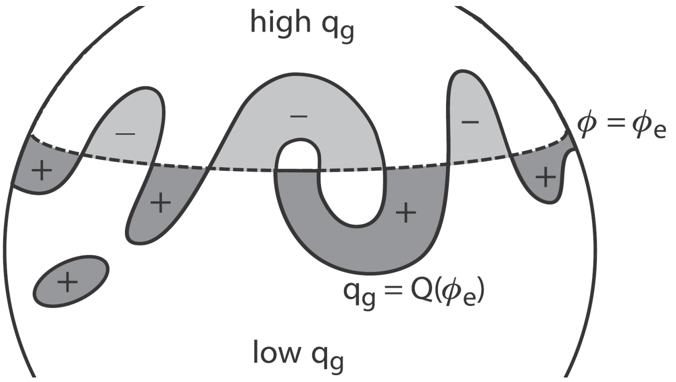

Figure 1: The basic idea of finite-amplitude wave activity: *Wave activity is defined as the difference in the surface integrals of potential vorticity (denoted here as q_g) over the dark gray area and the light gray area. Equivalent latitude ϕ_e (dashed contour) is chosen such that it encloses the same area as the wavy PV contour $q_g = Q$ (solid contour). The schematic is taken from Nakamura and Solomon (2010).*

diabatic contributions. Davies and Didone suggested that the traditional PV concepts of partition and attribution be applied to the advective tendencies of the PV error equation to further analyze different contributions to the error evolution (their section 3b). A partitioning of advective tendencies into contributions attributable to upper-level Rossby wave propagation and baroclinic interaction has been applied by Riemer and Jones (2010, 2014) in the context of Rossby wave evolution, following work by Davis et al. (1996). Their work considered also advective tendencies associated with the divergent flow as a proxy for the impact of latent heat release. Application of their partitioning in the context of error growth seems to be a promising way to separate out the baroclinic error growth from error propagation and error growth due to nonlinear processes.

Although the three-stage picture of Zhang et al. (2007) is conceptually very useful, there are indications that it is incomplete. Once the forecast errors have reached the synoptic scale, they can be expected to propagate like baroclinic wave packets (Hakim, 2005). This communicates errors and uncertainties over planetary-scale distances and makes the evolution sensitive to diabatic processes in the downstream region (Riemer and Jones, 2010). Indeed, several studies have shown that forecast errors and uncertainty can propagate along and grow within a Rossby wave packet (Anwender et al., 2008; Pantillon et al., 2013). The work by Rodwell et al. (2013) suggests that this chain of events plays an important role for occasional extremely poor forecasts of weather over Europe. One of the reasons behind this result may be that Europe lies at the end of the Atlantic storm track, where wave activity accumulates and leads to wave breaking (Gabriel and Peters, 2008; Masato et al., 2012). Taken together, these results suggest that one should add a fourth stage to the conceptual upscale-error growth model.

To understand the growth of errors from synoptic to planetary scales, it is necessary to diagnose the generation, propagation, and decay of Rossby wave packets. In the past, various methods have been applied for this purpose, based on envelope reconstruction of the meridional wind (Chang, 2000; Zimin et al., 2003, 2006; Glatt et al., 2011; Glatt and Wirth, 2014; Wolf and Wirth, 2015), on wave kinetic energy (Chang, 1999; Orlanski and Katzfey, 1991; Chang and Orlanski, 1993; Orlanski and Sheldon, 1995), or on wave activity fluxes derived from linear theory (Takaya and Nakamura, 1997, 2001; Nishii and Nakamura, 2004; Peters et al., 2007; Glatt et al., 2011). However, none of these approaches is able to distinguish between conservative propagation and diabatic modification and, thus, to pinpoint the key processes of uncertainty amplification in Rossby wave trains. Linear wave activity approaches are based on the neglect of higher-order terms, which unfortunately turned out not to be small.

A promising alternative are finite-amplitude versions of wave activity, which have recently been developed (Nakamura and Zhu, 2010; Nakamura and Solomon, 2010, 2011; Methven, 2013). The formulations of Nakamura and colleagues are based on the quasi-horizontal displacement of PV contours and adopt a hybrid Eulerian-Lagrangian framework to define the amplitude of eddies (Solomon and Nakamura, 2012). Fig. 1 illustrates the basic idea. The key difference with respect to linear wave activity is that there are no higher-order terms that have to be neglected. It follows that the

Figure 2: Emulation of upscale error growth *from convective uncertainty using a stochastic convection scheme. The black line (HR) shows results from a convection-permitting reference simulation. The green line (Tie) shows the overconfidence of the model at a ten times coarser resolution, when a standard convection scheme (Tiedtke) is used. The stochastic Plant-Craig scheme (PC, red line) however matches the high-resolution result very well.*

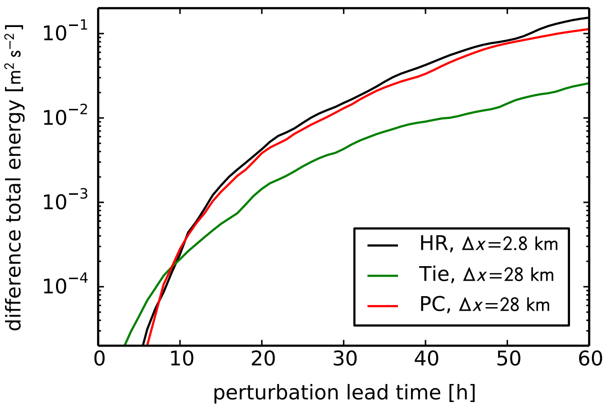

non-conservative term can readily be diagnosed. However, the wave activity of Nakamura et al. only provides information about the zonal mean state, which precludes an application to the zonal propagation of Rossby wave packets. An extension proposed in the current project aims to resolve this issue.

A1.3.2 Previous work

As described in this section, the project PIs have extensive experience with the study of atmospheric dynamics, the interaction of dynamics with diabatic heat sources, and the growth of errors. PI Craig started his career with a theoretical investigation of the interaction of baroclinic instability and cumulus convection (Craig and Cho, 1988), and later employed piecewise PV inversion to study the dynamics of a midlatitude cyclone with very strong latent heat release (Ahmadi-Givi et al., 2004), and the extratropical transition of a tropical cyclone (Agusti-Panareda et al., 2004). Using this method, it could be shown that the identifying characteristics of the newly described Type C cyclones (Deveson et al., 2002) could be explained by a combination of positive and negative feedbacks of latent heating on baroclinic instability (Plant et al., 2003). To represent the variability associate with convective clouds, a stochastic cumulus parameterization has been developed (Plant and Craig, 2008), and successfully implemented in the ICON global model where it was found that the variability of precipitation scales correctly with the model resolution (Keane et al., 2014). This modeling framework will be used in the project proposed here. In the research group PANDOWAE, Selz and Craig (2015) examined error growth in the COSMO model, using disturbance kinetic energy and other diagnostics to trace how the perturbations grow upscale and evolve into geostrophically balanced states that can continue to grow through baroclinic instability. Very recently we have demonstrated the feasibility of doing similar experiments in a model with coarser resolution and finding that the same upscale error growth is obtained when using the stochastic convection scheme of Plant and Craig (2008) to represent the convective scale variability (Fig. 2, manuscript in preparation). This opens the exciting possibility of investigating upscale error growth from convective to planetary scale without the extreme computational demands of a global cloud-resolving model.

PI Riemer has investigated the processes that contribute to the excitation, propagation, and amplification of Rossby-wave-type disturbances of the midlatitude jet during extratropical transition in a series of idealized numerical experiments (Riemer et al., 2008; Riemer and Jones, 2010, 2014) and for real-atmospheric cases (Riemer et al., 2014). Divergent outflow aloft was found to play an important role for the excitation and also for the downstream dispersion. Bifurcation points in the steering flow partly explained the low predictability associated with extratropical transition, and it has been demonstrated that this low predictability propagates into the downstream region, too. The PV-θ framework employed in these studies has been extended in the PI's PANDOWAE project to develop a quantitative diagnostic for the evolution of finite-amplitude, synoptic-scale Rossby waves. This diagnostic employs a Helmholtz decomposition of the flow and piecewise PV inversion under nonlinear balance (Davis, 1992; Charney, 1955) to partition advective tendencies into individual contributions representing Rossby wave propagation, baroclinic interaction, and upper-level divergent outflow. In addition, exploiting the unique YOTC data set (Waliser et al., 2012), the direct diabatic contribution was assessed. Results from this work indicate a large variability over individual troughs and ridges and emphasize the importance of the divergent flow, in particular for the amplification of ridges (Piaget et al., 2014, and ongoing PANDOWAE work). The diagnostic developed in PANDOWAE forms a basis for work proposed in WP 3. Advising two ongoing master theses, PI Riemer has also experience in assessing predictability of Rossby wave trains from ensemble data and investigating the dynamics of forecast errors in the PV-θ framework.

PI Wirth has extended and long-time experience with atmospheric dynamics in general, and Rossby waves in particular. He published work on the relevance of Rossby waves for tracer distributions (Wirth, 1993), on the effect of diabatic heating (Wirth, 1995), and on Rossby wave breaking (Hauck and Wirth, 2001). In recent years, Rossby wave packets were one of his main research interests in connection with the research group PANDOWAE. He has proposed novel methods to diagnose Rossby wave packets (Glatt and Wirth, 2014; Wolf and Wirth, 2015) and conducted comparisons with other, more established methods (Glatt et al., 2011). The work of Wirth and Eichhorn (2014) finds a systematic connection between upper level Rossby wave trains and strong surface cyclones over Europe. Currently, one of his PhD students is working on forecast errors and predictability associated with Rossby wave packets as well as the utility of small-amplitude wave activity fluxes. Atmospheric dynamics plays also a central role in the teaching activities of PI Wirth (Wirth, 2003, 2014).

A1.3.3 Project-related publications

Selz, T., and G. C. Craig, 2015: Upscale error growth in a high-resolution simulation of a summertime weather event over Europe. *Mon. Wea. Rev.*, doi:10.1175/MWR-D-14-00140.1, in press.

Keane, R. J., G. C. Craig, G. Zängl, and K. Keil, 2014: The Plant–Craig stochastic convection scheme in ICON and its scale adaptivity. *J. Atmos. Sci.*, **71**, 3404–3415.

Wirth, V. and J. Eichhorn, 2014: Long-lived Rossby wave trains as precursors to strong winter cyclones over Europe. *Quart. J. Roy. Met. Soc.*, **140**, 729–737.

Glatt, I. and V. Wirth, 2014: Identifying Rossby wave trains and quantifying their properties. *Quart. J. Roy. Met. Soc.*, **140**, 384–396.

Riemer, M. and S. C. Jones, 2014: Interaction of a tropical cyclone with a high-amplitude, midlatitude wave pattern: Waviness analysis, trough deformation and track bifurcation. *Quart. J. Roy. Meteor. Soc.*, **140**, 1362–1376.

Glatt, I., A. Dörnbrack, S. Jones, J. Keller, O. Martius, A. Müller, D. H. W. Peters, and V. Wirth, 2011: Utility of Hovmöller diagrams to diagnose Rossby wave trains. *Tellus* **63A**, 991–1006.

Riemer, M. and S. C. Jones, 2010: The downstream impact of tropical cyclones on a developing baroclinic wave in idealized scenarios of extratropical transition. *Quart. J. Roy. Meteor. Soc.*, **136**, 617–637.

Plant, J. M., and G. C. Craig, 2008: A stochastic parameterization for deep convection based on equilibrium statistics. *J. Atmos. Sci.*, **65**, 87-105.

Agusti-Panareda, A., C. D. Thorncroft, G. C. Craig, and S. L. Gray, 2004: The extratropical transition of hurricane Irene (1999): A potential vorticity perspective. *Quart. J. Roy. Meteor. Soc.*, **130**, 1047-1074.

Ahmadi-Givi, F., G. C. Craig and R.S. Plant, 2004: The dynamics of a mid-latitude cyclone with very strong latent heat release. *Quart. J. Roy. Meteor. Soc.*, **130**, 295-324.

A1.4 Research plan

A1.4.1 Objectives

In this project, a unified description of error growth from the convective to the hemispheric scale will be developed. This will be achieved by examining the growth and propagation of flow perturbations in numerical simulations and archived analysis data. New and improved diagnostic tools will be developed to quantify upscale uncertainty propagation, identify the physical processes that lead to their amplification and compare it to other sources of uncertainty. The objectives of the project are:

- Revisiting upscale error growth over a wide range of spatial scales from convective uncertainty to hemispheric saturation
- Seeking evidence for the hypothesized fourth stage of upscale error growth at the large-scale end that involves propagation and breaking of wave packets
- Assessing the practical importance of upscale error growth for medium-range weather forecasts
- Identification of bifurcation regions in the synoptic flow, and evaluation of the magnitude and mechanisms by which diabatic heating acts to perturb these regions
- Reconciliation of the piecewise PV and nonlinear wave activity perspectives regarding the impact of local disturbances on the synoptic- and planetary-scale flow.

A1.4.2 Work program

Strategy

The project combines the expertise of three groups at two universities with experience covering the different physical processes and scales of motion. An experienced Postdoc at LMU, responsible for WP 1–2 and supervised by PI Craig, will develop a global ensemble on selected case studies using the ICON model with a stochastic convective parameterization and a high-resolution subdomain. These simulations will be used to quantify the upscale growth and dynamical evolution of errors with diagnostics such as disturbance kinetic energy. Tools developed by the JGU partners will also be applied to the simulations and the convective and mesoscale processes in the ICON ensemble will be evaluated using high-resolution COSMO simulations, taking advantage of the methods shared in the CCA Ensemble Tools. At JGU, a PhD student under the supervision of PI Riemer (WP 3) will use piecewise PV inversion to describe the growth and evolution of perturbations in terms of PV building blocks. Physical mechanisms will be identified that lead to rapid spread of the forecast ensemble on synoptic scales. A second PhD student at JGU, this time supervised by PI Wirth and responsible for WP 4, will develop a new and improved wave activity diagnostic that will provide an alternative measure of the relative impact of diabatic and synoptic-scale dynamical processes. This view will be compared to the PV building block approach to characterize the strengths and weaknesses of the new approach. The three groups will work jointly together by applying their different methods and expertise to a common set of case studies to achieve a unified picture of error growth across scales.

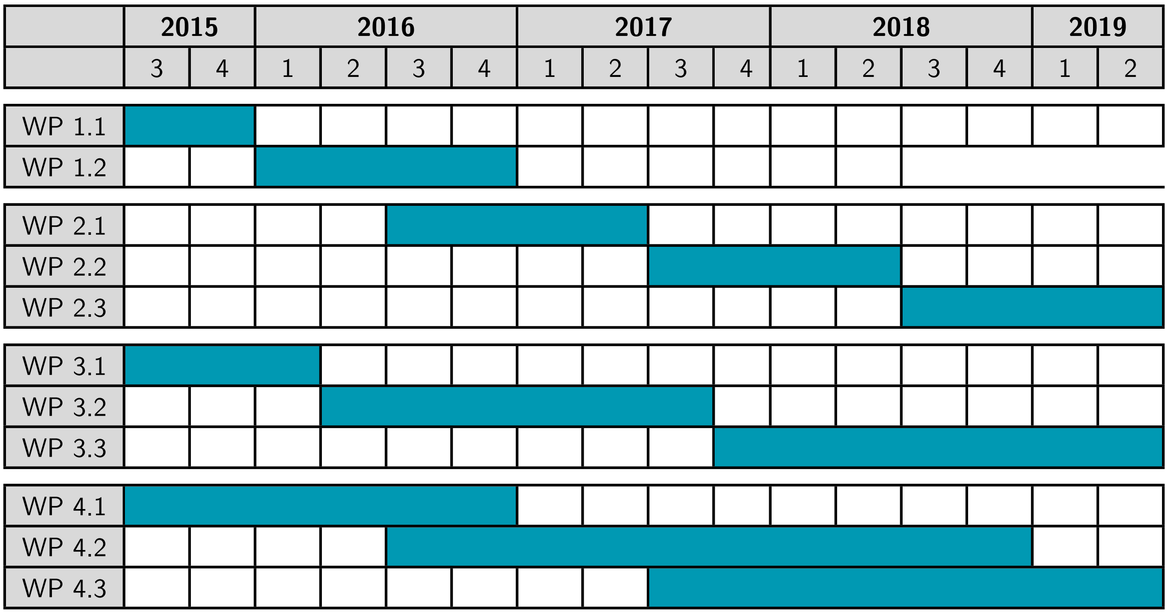

Workpackage 1: Upscale error growth paradigm

This workpackage will examine basic mechanisms and characteristics of upscale error growth from convective uncertainty up to global saturation, enabled by recent progress in the stochastic parameterization of convection. This work package will use the new global ICON model of DWD (Zängl et al., 2014). This model is uniquely suited since it is the only global model at present with an implementation of the Plant-Craig stochastic convection scheme that can accurate represent upscale error growth from convective to synoptic scales (Keane et al., 2014).

Task 1.1: Basic implementations, calibration and setup

In the first task the ICON model code will be extended to match the requirements of the project and to establish the basis for the joint evaluation. The Plant-Craig scheme (PC), which will be used to emulate convective scale uncertainty, has already been integrated into ICON (Keane et al., 2014). However, a careful calibration of its parameters has not yet been performed and, in addition, the scheme has not yet been tested with ICON at the resolution intended here (about 20 km). The simulations from Selz and Craig (2015) and from ongoing work (cf. Fig. 2) will be used as a reference to adjust basic properties of the convection scheme such as precipitation amount and partitioning.

For the error growth experiments proposed in this project some extensions of the PC implementation in ICON will be necessary: First, the possibility of changing the random-number seed during the model run at a desired time step has to be implemented. Second, bit-reproducibility of the model simulations is essential for error growth experiments. Therefore the assignment of random numbers to individual gridpoints must be independent of the parallelization configuration, which requires some effort given the unstructured icosahedral grid of ICON. Third, a bit-reproducible restart option of simulations with the PC scheme is not yet possible and will be implemented. Finally, in the current version of ICON basic output variables essential for this project like potential vorticity or some diabatic tendencies are still missing. In cooperation with DWD the missing code parts will be added to ICON in this task.

Task 1.2: Four generic simulations of upscale error growth

As an extension to Selz and Craig (2015) it is planned in this task to investigate the basic mechanism of upscale error growth from convective uncertainty up to global saturation with ICON. To reduce the computational effort to a manageable amount the Plant-Craig stochastic convection scheme will be used as an emulator for convective-scale uncertainty at a resolution around 20 km. First, four cases will be investigated, one in each season, selected in cooperation with other W2W projects. Especially, cases with campaign data available will be considered (A3). For each of the selected cases, simulations will be carried out with two different realizations of the Plant-Craig scheme: After a common spin-up time interval, the random seed of the scheme will be changed in one of the realizations resulting in a generation of a randomly displaced version of the convective clouds in that run. The integration time of these two simulations will be extended until they have become decorrelated on all spatial scales and are two independent representation of the climate (presumably two to four weeks). Following Selz and Craig (2015), diagnostics including the kinetic energy of the difference wind field as function of length scale will be applied on global or midlatitude areas to further investigate the basic properties of upscale error growth beyond the synoptic scale. The four cases will enable us to look for seasonal and hemispheric differences and, since the whole globe is covered, will contain the full range of weather phenomena, such as warm conveyor belts or mesoscale convective systems.

Data and basic quantitative results of these first ensemble simulations will be passed to the project partners at JGU and will be further studied there in Task 3.2 and Task 4.2 by attributing physical processes to the perturbation tendencies and by investigating development and divergence of Rossby wave trains. Together we will identify basic mechanisms and conditions for rapid upscale error growth and investigate the possibility of defining a fourth stage of error growth beyond the classic baroclinic instability at scales above the synoptic-scale.

Workpackage 2: Practical importance of upscale error growth

In this workpackages, experiments will be designed and performed that will enable us to clarify the practical importance of upscale error growth and its regime dependence, i. e., to compare it against other sources of uncertainty, to look for potentially vulnerable atmospheric states and to identify important and unimportant uncertainties. The ICON simulations from WP 1 will serve as a starting point, but we will also make use of archived data from the ECMWF Ensemble Prediction System (EPS). This system represents initial condition uncertainty through an ensemble data assimilation system that prepares 25 different analyses using perturbed observations and model physics (Isaksen et al., 2010). Model errors during the forecasts are represented by stochastically perturbing the tendencies produces by the physical parameterizations, including, but not limited to, convection (Palmer et al., 2009). The amplitude and space-time scales of the stochastic perturbations have been carefully tuned to give a good spread-skill relationship. The global model experiments will also be compared with results from the COSMO model, taking advantage of developments by other projects in W2W integrated in the CCA Ensemble Tools.

Task 2.1: Synoptic-scale uncertainty versus upscale error growth

The aim of this task is a comparison of the amplitudes of upscale grown errors from convection to the larger-scale uncertainties that develop from errors already present in the initial conditions due to an imperfect measurement- and data assimilation system. Therefore the small ensembles considered in WP 1 or a potentially most interesting subset of them will be extended to not only address different realizations of the convection but also initial condition uncertainty. To get a reasonable estimate of the initial condition uncertainty the ten member analysis from ECMWF's ensemble data assimilation system will be used to initialize the ICON model. From this sample we first carry out ten runs using the standard Tiedtke convection scheme or a deterministic version of the Plant-Craig scheme. Since these ICON ensembles are neither inflated by singular vector perturbations nor stochastic physics methods we expect them to be highly underdispersive and overconfident. Verifications of the probabilistic properties will be done by comparison with the ECMWF analysis or the well-calibrated ECMWF ensemble forecasts.

After that two different realizations of the Plant-Craig stochastic convection scheme will be added to the ensemble which again will be started from the ten member initial state uncertainty sample, resulting in a 30 member ensemble for each considered case. In contrast to the carefully tuned stochastic physics method used at ECMWF the Plant-Craig convection scheme represents only a single physical source of uncertainty. Thus the ICON ensembles carried out here allow us to assess the impact of convective uncertainty on medium-range forecasts. It will be evaluated to what extent the ensemble spread increases and how much of the ensemble overconfidence can be addressed by the use of the stochastic convection scheme. Spread-error relations will be computed, although the number of cases may be too small to yield reliable results.

A localized version of the disturbance kinetic energy diagnostics described in Selz and Craig (2015) will be used to detect regions and points in time with fast ensemble divergence and to identify the most divergent ensemble members. We expect effects of upscale error growth to be negligible in regions such as fronts, where latent heat release is controlled by the synoptic flow, but about equal to the uncertainty attributable to synoptic-scale errors in highly convective regimes with weak synoptic forcing. Again these most interesting runs will be further investigated at JGU with their PV-θ and wave-activity diagnostics in Task 3.3 and 4.2.

Task 2.2: Convection and synoptic-scale instability
In this task we will identify and investigate atmospheric states that are potentially very vulnerable to upscale error growth from convective uncertainty: The hypothesis will be tested that a high uncertainty in the convective mass flux particularly degenerates the forecast if it coincides with a region that also shows high sensitivity of the geostrophic flow. This may occur for example in prefrontal convection within a narrow ridge close to a growing cyclone. To detect such weather regimes, diagnostics for both properties are required. A standard tool to assess the synoptic-scale sensitivity are the singular vector amplitudes from the ECMWF adjoint model. Alternatively regions of high divergence in the ECMWF ensemble at short forecast lead times (12–24 h) could be used, which basically result from the ensemble inflation by singular vectors. Both diagnostics are available in the archive. The uncertainty of the convective mass flux can be assessed using the convective adjustment timescale (Done et al., 2006) that identifies when convection is strongly controlled, i. e., in equilibrium, with the synoptic flow. This diagnostic has not been used previously for output from numerical models with parameterized convection, since the parameterization typically assumes equlibrium convection and adjusts the model atmosphere accordingly. It is claimed however, that the most recent versions of the ECMWF convection can represent non-equilibrium convection (Bechtold et al., 2014), which would open the possibility of using the adjustment timescale diagnostic. But given the novelty of this application, a comparison will be performed first between calculations of the convective timescale from convection-permitting COSMO-DE forecasts and coarser ECMWF forecasts.

After that, both diagnostics will be calculated from archive data for a whole summertime period and for each day the weather situation over a selected source region will be divided into five different categories: (i)–(iv) equilibrium/non-equilibrium convection and sensitive/insensitive flow and (v) no convective activity. Germany could be a possible choice for such a region and here COSMO-DE forecasts can be used to calculate the convective timescale. If however this calculation turns out to work also on the coarser ECMWF forecasts we will be free to choose the source region. The results of Rodwell et al. (2013) suggest to choose the North-American continent from which perturbation will propagate downstream and amplify to generate the maximum impact on the weather in Europe (the target region).

Error growth experiments will be done after simulating selected cases of the categories (i)–(iv) and uncertainty growth will be investigated. Especially the resulting downstream-propagating variability will be compared and related to the categorization of the initial weather conditions in the source region. Therefore the convective mass flux in the source region will be perturbed, which can be done in two different ways: First, parameters of the Plant-Craig convection scheme can be modified to directly vary the mass flux. This method is easy and computationally cheap and will be used for a first set of experiments. However, the mass flux variability here is predetermined and does not necessarily correspond to its real uncertainty. Hence in a second set of experiments the grid of the ICON model in the considered region will be refined to a convection-permitting resolution. We expect from previous experiments (Selz and Craig, 2015) that the model will generate the mass flux variability automatically from simple noise perturbations when the convective time scale in the area is high. As for the ensembles generated in Task 1.2 and 2.1, a more qualitative assessment of the uncertainty propagation will be gained in cooperation with JGU for a selected subset of cases (Task 3.3 and 4.2).

Task 2.3: Sensitive parameters for upscale error growth
The previous tasks have considered the impact of directly forced variation of the distribution and amount of convective-scale latent heat release on the downstream weather development. In the final task of this workpackage it is planned to further investigate sensitivities of latent heat release to uncertainties from poorly known or unresolved processes below or near the convective scale and to assess their importance for downstream weather development with the help of the previous results. Three potential sources of uncertainty will be considered: (i) Moisture variability in the boundary layer, (ii) upscale impacts of boundary layer variability at the grid-scale and (iii) variations in cloud-microphysics parameters. The focus of this workpackage is on scales below and up to the synoptic scale which means that limited area model simulations are sufficient. We thus plan to use the COSMO model here, since it facilitates the integration of tools by other projects (mostly developed for COSMO) into our ensemble system. Three cases will be selected that have been investigated in the previous workpackages: A convective event in equilibrium, a convective event in non-equilibrium and a non-convective warm conveyor belt. In each case a multi-ensemble of forecasts will be generated by representing the uncertainties mentioned in (i)-(iii). The moisture field will be directly modified in the initial condition. Both, changing the amount of moisture as well as redistributing it according to the results of Fischer et al. (2013) will be considered. For (ii) the stochastic boundary layer scheme developed in Project A6 will be used to sample upscale impacts from boundary layer variability at the grid-scale that is usually not considered. Reasonable variations of microphysical parameters will be selected in agreement with results from Project B1. Initially, each source of uncertainty will be sampled separately but depending on the results and available computational resources also combinations of (i)-(iii) will be sampled.

Based on this ensemble we will perform a regime-dependent analysis of which of the sampled uncertainties lead to a significant ensemble spread contribution (cf. Groenemeijer and Craig, 2012). The results will enable the construction of future ensemble systems that could be designed to adapted their configuration to the prevailing weather regime and target region.

Workpackage 3: PV-θ framework for upscale growth and amplification
This workpackage will combine the quantitative PV-θ diagnostic for Rossby wave dynamics developed during PANDOWAE and the tendency equation for forecast errors derived by Davies and Didone (2013). The combined diagnostic is used to assess in detail the processes governing the upscale growth of forecast error and of ensemble spread.

Task 3.1: Optimization of the underlying PV inversion code
This preliminary task will improve the PV inversion code underlying the PV-θ diagnostic and adopt it to ICON data. PV inversion requires the solution of a three-dimensional, nonlinear, elliptical equation. The current inversion code uses a successive-overrelaxation scheme, the standard scheme until the 1970s. This scheme provides robust solutions but is computationally rather inefficient for the large domains desirable to investigate upscale growth to the near-hemispheric scale. Our investigations in an ensemble framework will require a large number of PV inversions and thus it seems worthwhile to dedicate some time early during this project to improve the inversion scheme such that subsequent research can be performed more efficiently. We will implement an inversion code based on multigrid methods, one of the current standard methods for large elliptical problems (Press et al., 1992, chapter 19.6). Furthermore, we will attempt to reduce the inversion problem from three to two dimensions

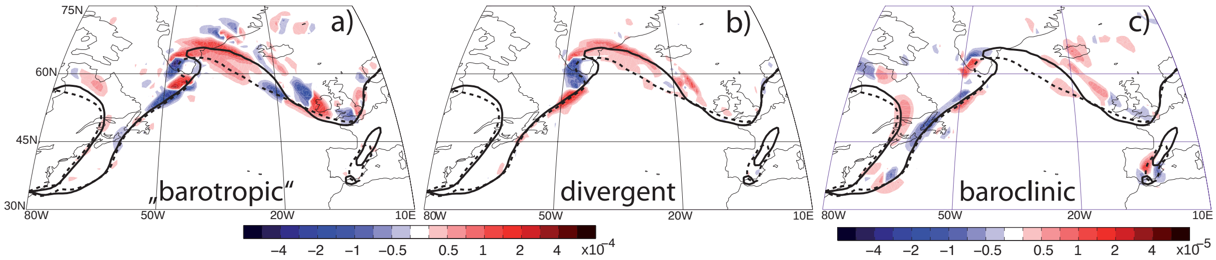

Figure 3: Decomposition of advective tendencies can be used to analyze individual contributions to the evolution of forecast errors. *Panels (a), (b), (c) show the contribution attributable to Rossby wave propagation, the divergent flow, and baroclinic interaction, respectively, to the material tendency of PV forecast errors on 320 K (shaded, in PVU s^{-1}, note the different scales of the color bars) over the North Atlantic for a 48 h forecast (initialized on 00 UTC 11 December 2013). The tendencies are calculated from the adiabatic version of Eq. (6) in Davies and Didone (2013) using the decomposition of the advective tendencies from our diagnostic developed in PANDOWAE. For reference, the solid (dashed) contour depicts the PV = 2 PVU isoline in the analysis (forecast). The "barotropic" and the divergent component make prominent contributions to the amplification of the ridge error. The baroclinic component is subordinate and generally an order of magnitude smaller.*

by using a zonal Fourier representation of all fields in an inversion domain spanning all longitudes. An additional advantage of this approach is that inaccuracies associated with unknown boundary conditions in the zonal direction are eliminated. This workpackage will benefit from the advise of applied mathematicians, in particular Prof. Lukáčová, greatly facilitated by W2W.

Task 3.2: Error growth in prototypical synoptic scenarios
This task will investigate the evolution of forecast errors in prototypical synoptic scenarios, which can be considered as building blocks of more complex atmospheric flows. These scenarios will be selected from the ICON simulations performed in WP 1. Our analysis will commence when fairly localized, finite-amplitude error patterns have developed in the forecast after 36–48 h and will end with the approximate saturation of the error after 10–14 days. Error tendencies will be quantified in the PV-θ framework and attributed to distinct physical processes. The prototypical scenarios will comprise (1) the leading edge of downstream development, (2) baroclinic development comprising (i) maritime and (ii) continental cyclones, (3) equivalent-barotropic systems including (i) mature, vertically-stacked cyclone-trough systems and (ii) high-amplitude ridges/ blocks, and (4) (i) cyclonic and (ii) anticyclonic wave breaking, including (iii) cut-offs.

The PV error tendency equation of Davies and Didone (2013) will be evaluated on isentropic levels intersecting the midlatitude tropopause ($\sim$ 320 K). Applying our diagnostic developed in PANDOWAE, the wind is partitioned into non-divergent components associated with upper-level and lower-level PV anomalies[1] and into its irrotational component: $\vec{v} = \vec{v}_{bt} + \vec{v}_{bc} + \vec{v}_{div}$. As in previous work, the respective advective tendencies can be attributed to (i) quasi-horizontal ("barotropic") propagation of the (upper-level) Rossby wave, (ii) baroclinic coupling, and (iii) divergent upper-level outflow. The individual error tendencies are illustrated in Fig. 3 for a 48 h forecast with a prominent amplitude error in a ridge over the North Atlantic. The "barotropic" and the divergent component both amplify the ridge error at this time while the baroclinic interaction makes an overall minor contribution. This result hints to an avenue for error growth that is distinct to baroclinic growth in the popular 3-stage error growth model.

Error growth in the prototypical scenarios will then be characterized in terms of the individual contributions. The relative importance of individual processes will be quantified, the respective individual growth rates estimated and compared between scenarios. It will also be compared how fast the individual scenarios reach saturation. We will examine if localized errors exhibit propagation char-

[1] In our own previous work a separation level of 650 hPa for the PV anomalies has been proven useful.

acteristics of coherent wave packets, in particular in baroclinically stable versus unstable situations. Finally, we will seek to identify forecast error "graveyards", i. e., regions where downstream error propagation ceases and a putative error wave packet looses its spatial coherence.

Task 3.3: Evolution of ensemble spread in the PV-θ framework
This task will investigate the growth of ensemble spread over different forecast times applying the diagnostic described in Task 3.2. Ensembles from WP 2.1 and WP 2.2 will be considered. These workpackages will provide also information about ensemble spread and a measure of the divergence of individual members. We will start with the ensemble that generally exhibits the largest spread. To gain some intuition, we will first examine the evolution of the most diverging members. These members will be characterized by the individual contributions to error growth, as outlined in Task 3.2. To gain more robust results, the analysis will be repeated studying the composites of the most diverging quintiles. Both analyses will be performed for forecast times of 3, 5, 7, 10 and 14 days. Main foci of the analyses will be if the prominent divergence of ensemble members can be attributed to distinct processes, if these processes change with the forecast time, and if the divergence is a continuous process in the sense that the same ensemble members exhibit the largest divergence for all forecast times. Such an improved conceptual understanding of the evolution of forecast uncertainties may have important ramifications for the future interpretation and design of ensemble forecasts.

Finally, we will collaborate with A7 to explore the full potential of the spatio-temporal information contained in the ensembles. Techniques for feature inference in ensembles and feature similarity detection (WP 2 and WP 5 in A7, respectively) will be applied to obtain a more complete view on the spatio-temporal correlations between the PV error tendencies and the evolution of ensemble spread in a specified region. We will investigate the location and forecast time for which the different tendencies show the highest correlations. Envisioned results of this investigation are statements such as: "The ensemble spread of a 7-day forecast over Europe is governed predominantly by PV tendencies due to divergent flow associated with a Newfoundland cyclone between forecast days 3–5". It is anticipated that related collaboration will be continued in future phases of W2W.

Workpackage 4: Diagnosing large-amplitude Rossby wave packets

This workpackage will develop a novel diagnostic to detect and follow large-amplitude Rossby wave packets. The diagnostic should also provide a distinction between conservative wave propagation and nonconservative (diabatic) processes. The new tool will be applied to study the upscale propagation of errors on the large-scale end of the cascade.

Task 4.1: Development of a new diagnostic for large-amplitude eddies
The finite-amplitude formulations for wave activity of Nakamura and colleagues have many attractive features, but unfortunately they only provide information about the zonally averaged flow. In the current workpackage we start from the primitive-equations version of Nakamura and Solomon (2011) and generalize their concept through a "zonal disaggregation". This allows us to localize the eddies also in the zonal direction. In essence, our new method combines the advantages of the two earlier approaches, i. e., the zonal resolution of Takaya and Nakamura (2001) and the finite amplitude nature of Nakamura and Solomon (2011). The diagnostic will first be developed using ERA-Interim reanalysis data (Dee et al., 2011), but later it will be implemented into ICON in order to be able to use the same model data as the other workpackages.

We start with implementing Nakamura's original formulation for zonal mean wave activity. The latter implies a sum over a number of terms, some of which are positive and some of which are negative (see Fig. 1). Each term represents an entire trough or an entire ridge, i. e., one half wavelength of the eddy. The sum of all terms is positive by necessity, which guarantees that zonal mean wave activity is positive definite. Our algorithm will modify the individual terms in order to make them positive without changing their sum. At this stage the field still varies on the scale of individual troughs and ridges. Application of a zonal filter, denoted by $\langle ... \rangle$, finally results in a diagnostic which quantifies the strength of a finite-amplitude eddy as a smooth function of longitude (in addition to latitude and altitude). The filtered wave activity will be denoted by $\langle \mathcal{A} \rangle$. Considering various episodes we will study the typical appearance of finite amplitude wave packets and determine the optimum form of the filter.

Task 4.2: Application of the new diagnostic to quantify errors and uncertainties and the role of non-conservative processes

We will apply our new diagnostic $\langle \mathcal{A} \rangle$ from Task 4.1 to selected ICON-model simulations provided by WP 1, 2.1 and 2.2. This allows us to quantify the strength of finite amplitude eddies, thus providing information about the upscale end of the chain of events which will be considered in the other workpackages. We will compare the model forecasts with the verifying analyses on the level of our diagnostic in order to quantify errors associated with Rossby wave trains, their generation and their propagation. Similarly, we will apply the diagnostic to the ensembles generated in WP 2.1 and 2.2 in order to obtain information about uncertainties on the large-scale end of the spectrum.

Our new diagnostic opens the possibility to obtain information about the role of different processes in the build-up or decay of eddies, in particular the distinction between conservative propagation and non-conservative processes. To the extent that the latter are dominated by diabatic processes (like we expect, e. g., in a warm conveyor belt or a mesoscale convective complex), this allows, for the first time, to diagnose these processes on the level of wave activity. The main idea is to quantify the strength S of non-conservative processes through

$$\frac{\partial \langle \mathcal{A} \rangle}{\partial t} + \langle q' v' \rangle = \langle S \rangle \qquad (1)$$

as a residuum between $\partial \langle \mathcal{A} \rangle / \partial t$ and $\langle q' v' \rangle$, where the last two terms are explicitly computed from the model data. The eddy flux term $\langle q' v' \rangle$, in turn, can be partitioned into distinct parts through $v' = v'_{bt} + v'_{bc} + v'_{div}$, where each part represents a conservative process as described in more detail in WP 3 (see also Piaget et al., 2014).

We will explore to what extent our new diagnostic is able to quantify the role of conservative dynamics versus non-conservative processes. To this end we will analyze episodes which are considered by the other workpackages and which include strong diabatic processes. If successful, we will again compare the forecast with the verifying analysis, in order to obtain information which process is particularly fraught with error.

Task 4.3: Conceptual connection between the PV perspective and the wave activity perspective

As mentioned earlier, there is a conceptual dichotomy between the PV-perspective and the formulations in terms of wave activity and related fluxes. To some extent this has prevented progress in the past. We aim to advance our theoretical understanding by bridging this gap in the framework of the bartropic model. Model code will be provided by the partners at KIT.

The issue is illustrated in Fig. 4. Assume that originally the domain is free of waves [panel (a)] and that later a wave packet propagates into the domain [panel (b)]. The wave packet is associated with large-amplitude displacements of a the PV contours (blue lines) from their original positions. It is one of the key properties of the finite amplitude wave activity that the zonal wind must be reduced from its original value in areas of significant wave activity, such that the sum $\langle \mathcal{A} \rangle + \langle u \rangle$ remains constant [e. g., Eq. (15) in Nakamura and Zhu 2010]. This is depicted in panel b through the shorter green arrows within the area of the wave packet. At the same time, the wave packet is characterized by positive and negative PV anomalies (red plus/minus signs). Inversion of these PV anomalies produces circulation anomalies (red circles). The projection of these circulation anomalies onto the zonal direction at the equivalent latitude (dashed line) is equivalent to a reduction of the zonal wind. Thus, both perspectives produce qualitatively the same prediction, namely a reduction

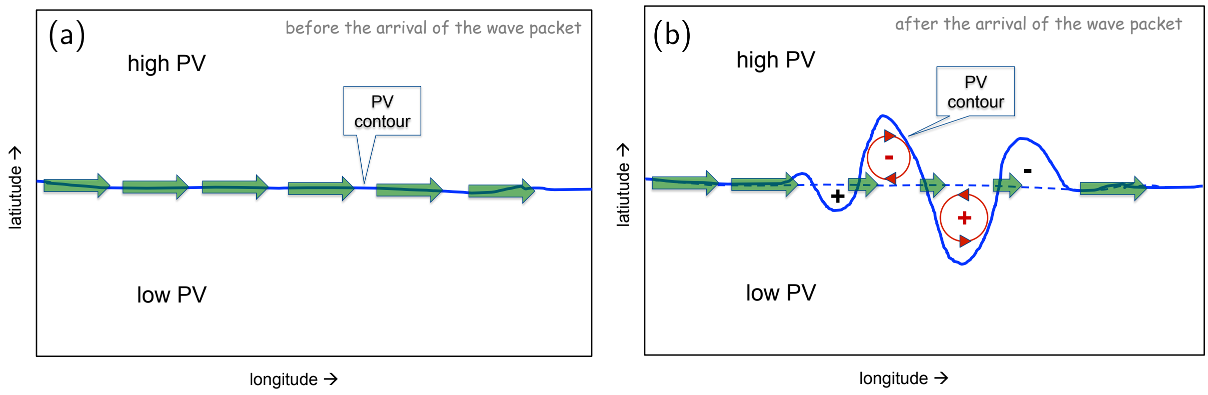

Figure 4: Schematic illustration for the conceptual unification between the PV-perspective and the wave activity perspective in the framework of the barotropic model. *Panel (a) represents the situation before the arrival of a wave packet, panel (b) the situation after the arrival of a wave packet. The wave packet displaces a given PV contour (solid blue line) from its original position (dashed blue line). The green arrows represent the zonal wind; the red circles in panel b with arrows and plus/minus signs represent PV anomalies together with the induced circulation anomalies.*

of the zonal wind in the neighborhood of local perturbations owing to the wave packet.

In the current task we will test the hypothesis that the above reasoning holds true for our new formulation of wave activity. To this end we will design an idealized model setup with flow over an isolated mountain, which produces a Rossby waves packet with gradual eastward propagation. The model code will then be enhanced by implementing our novel diagnostic $\langle \mathcal{A} \rangle$ as well as an option for piecewise PV inversion (Rosting and Kristiansson, 2012). Eventually we will compare the reduction of the zonal wind (smaller arrows in Fig. 4b) obtained from $\Delta \langle u \rangle = -\langle \mathcal{A} \rangle$ with those obtained from piecewise PV inversion. To the extent that both are similar, this provides a conceptional bridge between the wave activity and the PV perspective.

2 References

Agusti-Panareda, A., C. D. Thorncroft, G. C. Craig, and S. L. Gray, 2004: The extratropical transition of hurricane Irene (1999): A potential-vorticity perspective. *Quart. J. Roy. Meteor. Soc.*, **130**, 1047–1074.

Ahmadi-Givi, F., G. Graig, and R. Plant, 2004: The dynamics of a midlatitude cyclone with very strong latent-heat release. *Quart. J. Roy. Meteor. Soc.*, **130**, 295–323.

Anwender, D., P. A. Harr, and S. C. Jones, 2008: Predictability Associated with the Downstream Impacts of the Extratropical Transition of Tropical Cyclones: Case Studies. *Mon. Wea. Rev.*, **136**, 3226–3247.

Archambault, H. M., L. F. Bosart, D. Keyser, and J. M. Cordeira, 2013: A Climatological Analysis of the Extratropical Flow Response to Recurving Western North Pacific Tropical Cyclones. *Mon. Wea. Rev.*, **141**, 2325–2346.

Bechtold, P., N. Semane, P. Lopez, J.-P. Chaboureau, A. Beljaars, and N. Bormann, 2014: epresenting equilibrium and nonequilibrium convection in large-scale models. *J. Atmos. Phys.*, **71**, 734–753.

Chagnon, J., S. Gray, and J. Methven, 2013: Diabatic processes modifying potential vorticity in a North Atlantic cyclone. *Quart. J. Roy. Meteor. Soc.*, **139**, 1270–1282.

Chang, E. K. M., 1999: Characteristics of Wave Packets in the Upper Troposphere. Part II: Seasonal and Hemispheric Variations. *J. Atmos. Phys.*, **56**, 1729–1747.

Chang, E. K. M., 2000: Wave Packets and Life Cycles of Troughs in the Upper Troposphere: Examples from the Southern Hemisphere Summer Season of 1984/85. *Mon. Wea. Rev.*, **128**, 25–50.

Chang, E. K. M. and I. Orlanski, 1993: On the Dynamics of a Storm Track. *J. Atmos. Phys.*, **50**, 999–1015.

Charney, J., 1955: The use of the primitive equations of motion in numerical prediction. *Tellus*, **7**, 22–26.

Craig, G. and H.-R. Cho, 1988: Cumulus heating and CISK in the extratropical atmosphere. Part I: Polar lows and comma clouds. *J. Atmos. Phys.*, **45**, 2622–2640.

Davies, H. C. and M. Didone, 2013: Diagnosis and Dynamics of Forecast Error Growth. *Mon. Wea. Rev.*, **141**, 2483–2501.

Davis, C. A., 1992: Piecewise Potential Vorticity Inversion. *J. Atmos. Phys.*, **49**, 1397–1411.

Davis, C. A., E. D. Grell, and M. Shapiro, 1996: The balanced dynamical nature of a rapidly intensifying oceanic cyclone. *Mon. Wea. Rev.*, **124**, 3–26.

Dee, D. P., et al., 2011: The ERA-Interim reanalysis: configuration and performance of the data assimilation system. *Quart. J. Roy. Meteor. Soc.*, **137**, 553–597.

Deveson, A., K. Browning, and T. Hewson, 2002: A classification of FASTEX cyclones using a height-attributable quasi-geostrophic vertical-motion diagnostic. *Quart. J. Roy. Meteor. Soc.*, **128**, 93–117.

Dirren, S., M. Didone, and H. C. Davies, 2003: Diagnosis of "forecast-analysis" differences of a weather prediction system. *Geophys. Res. Lett.*, **30**, 2060.

Done, J., G. Craig, S. Gray, P. Clark, and M. Gray, 2006: Mesoscale simulations of organized convection: Importance of convective equilibrium. *Quart. J. Roy. Meteor. Soc.*, **132**, 737–756.

Durran, D. R. and M. Gingrich, 2014: Atmospheric Predictability: Why Butterflies Are Not of Practical Importance. *J. Atmos. Phys.*

Eady, E. T., 1949: Long waves and cyclone waves. *Tellus*, **1**, 33–52.

Fischer, L., G. Craig, and C. Kiemle, 2013: Horizontal structure function and vertical correlation analysis of mesoscale water vapor variability observed by airborne lidar. *J. Geophys. Res.: Atmos.*, **118**, 7579–7590.

Gabriel, A. and D. Peters, 2008: A Diagnostic Study of Different Types of Rossby Wave Breaking Events in the Northern Extratropics. *J. Meteor. Soc. Japan.*, **86**, 613–631.

Glatt, I., A. Dörnbrack, S. Jones, J. Keller, O. Martius, A. Müller, D. H. W. Peters, and V. Wirth, 2011: Utility of Hovmöller Diagrams to Diagnose Rossby Wave Trains. *Tellus*, **63A**, 991–1006.

Glatt, I. and V. Wirth, 2014: Identifying Rossby wave trains and quantifying their properties. *Quart. J. Roy. Meteor. Soc.*, **140**, 384–396.

Grams, C. M., S. C. Jones, C. A. Davis, P. A. Harr, and M. Weissmann, 2013: The impact of Typhoon Jangmi (2008) on the midlatitude flow. Part I: Upper-level ridgebuilding and modification of the jet. *Quart. J. Roy. Meteor. Soc.*, **139**, 2148–2164.

Grams, C. M., et al., 2011: The key role of diabatic processes in modifying the upper-tropospheric wave guide: a North Atlantic case-study. *Quart. J. Roy. Meteor. Soc.*, **137**, 2174–2193.

Gray, S., C. Dunning, J. Methven, G. Masato, and J. Chagnon, 2014: Systematic model forecast error in Rossby wave structure. *Geophys. Res. Lett.*, **41**, 2979–2987.

Groenemeijer, P. and G. Craig, 2012: Ensemble forecasting with a stochastic convective parametrization based on equilibrium statistics. *Atmos. Chem. Phys.*, **12**, 4555–4565.

Hakim, G. J., 2005: Vertical Structure of Midlatitude Analysis and Forecast Errors. *Mon. Wea. Rev.*, **133**, 567–578.

Hauck, C. and V. Wirth, 2001: Diagnosing the impact of stratospheric planetary wave breaking in a linear model. *J. Atmos. Phys.*, **58**, 1357–1370.

Hohenegger, C. and C. Schär, 2007a: Atmospheric predictability at synoptic versus cloud-resolving scales. *Bull. Am. Meteorol. Soc.*, **88**, 1783–1793.

Hohenegger, C. and C. Schär, 2007b: Predictability and error growth dynamics in cloud-resolving models. *J. Atmos. Phys.*, **64**, 4467–4478.

Isaksen, L., J. Haseler, R. Buizza, and M. Leutbecher, 2010: The new Ensemble of Data Assimilations. *ECMWF Newsletter*, **123**, 17–21.

Keane, R., G. C. Craig, C. Keil, and G. Zängl, 2014: The Plant-Craig stochastic convection scheme in ICON and its scale-adaptivity. *J. Atmos. Phys.*, **71**, 3404–3415.

Masato, G., B. J. Hoskins, and T. J. Woolings, 2012: Wave-breaking characteristics of midlatitude blocking. *Quart. J. Roy. Meteor. Soc.*, **138**, 1285–1296.

Methven, J., 2013: Wave activity for large-amplitude disturbances described by the primitive equations on the sphere. *J. Atmos. Phys.*, **70**, 1616–1630.

Nakamura, N. and A. Solomon, 2010: Finite-amplitude wave activity and mean flow adjustments in the atmospheric general circulation. *J. Atmos. Phys.*, **67**, 3967–3983.

Nakamura, N. and A. Solomon, 2011: Finite-Amplitude Wave Activity and Mean Flow Adjustments in the Atmospheric General Circulation. Part II: Analysis in the Isentropic Coordinate. *J. Atmos. Phys.*, **68**, 2783–2799.

Nakamura, N. and D. Zhu, 2010: Finite-Amplitude Wave Activity and Diffusive Flux of Potential Vorticity in Eddy-Mean Flow Interaction. *J. Atmos. Phys.*, **67**, 2701–2716.

Nishii, K. and H. Nakamura, 2004: Tropospheric influence on the diminished Antarctic ozone hole in September 2002. *Geophys. Res. Lett.*, **31**, L16 103.

Orlanski, I. and J. Katzfey, 1991: The Life Cycle of a Cyclone Wave in the Southern Hemisphere. Part I: Eddy Energy Budget. *J. Atmos. Phys.*, **48**, 1972–1998.

Orlanski, I. and J. P. Sheldon, 1995: Stages in the energetics of baroclinic systems. *Tellus*, **47A**, 605–628.

Palmer, T., R. Buizza, F. Doblas-Reyes, T. Jung, M. Leutbecher, G. Shutts, M. Steinheimer, and A. Weisheimer, 2009: Stochastic parametrization and model uncertainty. *Tech. Rep. ECMWF RD Tech. Memo.*, **598**, 42 pp.

Pantillon, F., J.-P. Chaboureau, C. Lac, and P. Mascart, 2013: On the role of a Rossby wave train during the extratropical transition of hurricane Helene (2006). *Quart. J. Roy. Meteor. Soc.*, **139**, 370–386.

Peters, D., P. Vargin, and H. Körnich, 2007: A Study of the Zonally Asymmetric Tropospheric Forcing of the Austral Vortex Splitting During September 2002. *Tellus*, **59A**, 384–394.

Piaget, N., P. Froidevaux, P. Giannakaki, F. Gierth, O. Martius, M. Riemer, G. Wolf, and C. M. Grams, 2014: Dynamics of a local Alpine flooding event in October 2011: moisture source and large-scale circulation. *Quart. J. Roy. Meteor. Soc.*, doi:10.1002/qj.2496, in press.

Plant, R. and G. Craig, 2008: A stochastic parameterization for deep convection based on equilibrium statistics. *J. Atmos. Phys.*, **65**, 87–105.

Plant, R., G. Craig, and S. Gray, 2003: On a threefold classification of extratropical cyclogenesis. *Quart. J. Roy. Meteor. Soc.*, **129**, 2989–3012.

Press, W. H., B. P. Flannery, S. A. Teukolsky, and W. T. Vetterling, 1992: *Numerical Recipes. The Art of Scientific Computing*. Cambridge University Press, 2nd edition, 818 pp.

Riemer, M., M. Baumgart, and S. Eiermann, 2014: Cyclogenesis downstream of extratropical transition analyzed by Q-vector partitioning based on flow geometry. *J. Atmos. Phys.*, **71**, 4204–4220.

Riemer, M. and S. C. Jones, 2010: The downstream impact of tropical cyclones on a developing baroclinic wave in idealized scenarios of extratropical transition. *Quart. J. Roy. Meteor. Soc.*, **136**, 617–637.

Riemer, M. and S. C. Jones, 2014: Interaction of a tropical cyclone with a high-amplitude, midlatitude wave pattern: Waviness analysis, trough deformation and track bifurcation. *Quart. J. Roy. Meteor. Soc.*, **140**, 1362–1376.

Riemer, M., S. C. Jones, and C. A. Davis, 2008: The impact of extratropical transition on the downstream flow: An idealized modelling study with a straight jet. *Quart. J. Roy. Meteor. Soc.*, **134**, 69–91.

Rodwell, M. J., et al., 2013: Characteristics of occasional poor medium-range weather forecasts for Europe. *Bull. Am. Meteorol. Soc.*, **94**, 1393–1405.

Rosting, B. and J. E. Kristiansson, 2012: The Usefulness of Piecewise Potential Vorticity Inversion. *J. Atmos. Phys.*, **69**, 934–941.

Selz, T. and G. Craig, 2015: Upscale error growth in a high-resolution simulation of a summertime weather event over Europe. *Mon. Wea. Rev.*, doi:10.1175/MWR-D-14-00140.1, in press.

Solomon, A. and N. Nakamura, 2012: An exact Lagrangian-mean wave activity for finite-amplitude disturbances to barotropic flow on a sphere. *J. Fluid Mech.*, **693**, 69–92.

Takaya, K. and H. Nakamura, 1997: A formulation of a wave-activity flux for stationary Rossby waves on a zonally varying basic flow. *Geophys. Res. Lett.*, **24**, 2985–2988.

Takaya, K. and Y. Nakamura, 2001: A Formulation of a Phase-Independent Wave-Activity Flux for Stationary and Migratory Quasigeostrophic Eddies on a Zonally Varying Basic Flow. *J. Atmos. Phys.*, **58**, 608–627.

Waliser, D. E., et al., 2012: The "year" of tropical convection (May 2008–April 2010): Climate variability and weather highlights. *Bull. Am. Meteorol. Soc.*, **93**, 1189–1218.

Wirth, V., 1993: Quasi-stationary planetary waves in total ozone and their correlation with lower stratospheric temperature. *J. Geophys. Res.: Atmos.*, **98**, 8873–8882.

Wirth, V., 1995: Diabatic heating in an axisymmetric cut-off cyclone and related stratosphere-troposphere exchange. *Quart. J. Roy. Meteor. Soc.*, **121**, 127–147.

Wirth, V., 2003: Potentielle Vorticity in der Dynamischen Meteorologie. Lecture notes.

Wirth, V., 2014: Atmospheric Dynamics. Lecture notes. Available from the author upon request.

Wirth, V. and J. Eichhorn, 2014: Long-lived Rossby wave trains as precursors to strong winter cyclones over Europe. *Quart. J. Roy. Meteor. Soc.*, **140**, 729–737.

Wolf, G. and V. Wirth, 2015: Implications of the semigeostrophic nature of Rossby waves for Rossby wave packet detection. *Mon. Wea. Rev.*, **143**, 26–38.

Zängl, G., D. Reinert, P. Rípodas, and M. Baldauf, 2014: The icon (icosahedral non-hydrostatic) modelling framework of dwd and mpi-m: Description of the non-hydrostatic dynamical core. *Quart. J. Roy. Meteor. Soc.*, doi:10.1002/qj.2378, in press.

Zhang, F., N. Bei, R. Rotunno, C. Snyder, and C. C. Epifanio, 2007: Mesoscale predictability of moist baroclinic waves: Convection-permitting experiments and multistage error growth dynamics. *J. Atmos. Phys.*, **64**, 3579–3594.

Zimin, A. V., I. Szunyogh, B. R. Hung, and E. Ott, 2006: Extracting Envelopes of Nonzonally Propagating Rossby Wave Packets. *Mon. Wea. Rev.*, **134**, 1329–1333.

Zimin, A. V., I. Szunyogh, D. J. Patil, B. R. Hunt, and E. Ott, 2003: Extracting Envelopes of Rossby Wave Packets. *Mon. Wea. Rev.*, **131**, 1011–1017.